 https://doi.org/10.3311/PPci.21260

Periodica Polytechnica Civil Engineering, 67(2), pp. 552–560, 2023

Evaluating the Cyclic Behavior of the Sloped Extended End-plate Beam-to-column Connections

Mirreza Miryahyavi[1], Reza Khani[1*], Yousef Hosseinzadeh[1]

[1] Department of structural Engineering, Faculty of Civil Engineering, University of Tabriz, 29 Bahman Blvd., 5166616471, Tabriz, Iran
[*] Corresponding author, e-mail: r.khani@tabrizu.ac.ir

Received: 30 September 2022, Accepted: 29 January 2023, Published online: 17 February 2023

Abstract

In the Northridge and Kobe earthquakes, brittle failure of the welded beam-to-column connections was observed in steel structures. So, bolted connections were considered as an alternative to these kinds of connections. Extended end-plate beam-to-column connection is one of the most commonly used connections in steel structure. In this article, the behavior of the sloped extended end-plate beam-to-column connections is studied. Finite element method was used to investigate the behavior of the connection by ABAQUS software. The main aim of the study was to investigate the cyclic behavior of the four beam-to-column connections with beam angles of 0, 10, 15, and 20 degrees with respect to horizon. Also, the behavior of the mentioned connections was compared with extended end-plate connections with perpendicular angle. Results showed that the ductility and moment-resisting capacity of the sloped extended end-plate beam-to-column connections decrease by increasing beam angle, but rotational and moment-resisting capacities of the models satisfy the limitation of the design codes such as 0.04 drift limit for bearing capacity before failure.

Keywords

cyclic behavior, extended end-plate connection, sloped moment connection, finite element model, hysteresis

1 Introduction

Moment Resisting Frame (MRF) is one of the most useful systems in steel structures against earthquake loads in which connections play the main role in bearing lateral loads [1]. Therefore, it is essential to apply connections which are beneficial in both financial and performance aspects against seismic loads. Due to the occurrence of the Northridge and Kobe earthquakes and failure of the connections, researchers decided to adopt some new considerations [2]. Investigations showed that the brittle failure of beam-to-column welded connection is the main reason for steel structures damage [3, 4]. Comparing bolted and welded connections shows that bolted connections are better and more ductile than welded ones which provide high energy dissipation capacity [5]. Therefore, to improve steel structures ductility, researchers suggested bolted connections like the prequalified connections in AISC 358 [6].

Determining column and beam cross-sections needs considering the behavior of the connection. Connections are classified as hinged, semi-rigid, and rigid based on their stiffness [7]. In hinged connections, there is no restriction on the rotation of the connection, and no moment transfers between the connection. Also, the rigidity of the connection is negligible resulting in large rotation of the connection. However, semi-rigid connections experience not only shear force but also moment. Therefore, the rotation of the connection is less than hinged connections. In a frame with semi-rigid connections, moments at the middle and two ends of the beam are close to each other leading to the moment balance and optimized cross-sections of the elements. Using the strong column-weak beam concept is one of the advantages of the semi-rigid connections [8]. Using this concept results in smaller beam cross-section and lateral displacement of the frame than hinged connections [9]. On the other hand, Due to the high rigidity of the rigid connections, in these types of connections moments are transferred between elements. Also, the angles between the elements are fixed both before and after applying force. Rigid connections can be welded and bolted, so common pre-qualified connections are incorporated in AISC 358 [6] such as RBS (Reduced Beam Section) [10], BUEEP (Bolted Unstiffened Extended End-Plate) [11], BSEEP (Bolted Stiffened Extended End-Plate) [12], and WFP (Welded Flange Plate) [13].

Cite this article as: Miryahyavi, M., Khani, R., Hosseinzadeh, Y. "Evaluating the Cyclic Behavior of the Sloped Extended End-plate Beam-to-column Connections", Periodica Polytechnica Civil Engineering, 67(2), pp. 552–560, 2023. https://doi.org/10.3311/PPci.21260

Krishnamurthy [14] recommended an economical and safe design procedure for end-plate connections for beam-to-column connections and investigated head plate thickness effect on these connections. Ghassemieh et al. [15] proposed a design procedure for the stiffened extended end-plate connection containing two rows of bolt on each side of tension part. Adey et al. [16] carried out an experimental study on 15 extended end-plate connections under cyclic load to obtain significant design parameters. The results indicated the potential of the extended end-plate connections to be used in seismic regions. Sumner and Murray [17] studied the design and the behavior of the end-plate beam-to-column connection under cyclic loads by testing six specimens. The results showed that extended end-plate connections are able to satisfy the requirements.

Diaz et al. [18] have studied a 3D model of the end-plate beam-to-column connection in ANSYS software. It was concluded that material hardening and plates interaction parameters have the most important effects on the connection behavior. Dessouki et al. [19] developed a 3D finite element model to assess the non-linear behavior of the extended end-plate connections using four bolts and multiple row extended end plates. They evaluated the effect of various parameters such as end-plate thickness, bolt pitch, beam depth, bolts diameter, end-plate stiffener and bolts gage by doing parametric study. Yang et al. [20] conducted a 3D nonlinear finite element analysis on five rigid connection samples to evaluate energy dissipation capacity, connection ductility, and applicability according to South Korean codes.

di Sarno et al. [21] conducted a numerical study on the case studies in Amatrice, Central Italy, which were moment resisting frame buildings and suggested possible improvements. Cyclic performance of post-Northridge welded connections was assessed by Yilmaz and Bekiroglu [22] in ANSYS software. Reduced Beam Section (RBS), Welded Unreinforced Flange – Welded Web (WUF-W), and Welded Flange Plate (WFP) connections were evaluated, and it was concluded that high stiffness and high safety belong to WFP and RBS connections, respectively. Llanes-Tizoc et al. [23] numerically investigated the reliability of 3D steel buildings under seismic load by obtaining fragility curves and median values of the maximum drifts. The Results showed an improvement in the structural reliability and important effect of the stiffness and energy dissipation on the mentioned outputs.

Design standards provide some prequalified connections for intermediate and special moment resisting frames connecting orthogonally the beam to the column. Recently, some researchers studied about sloped beam-to-column connections concept. For example, Mashayekh and Uang [24] conducted an experiment on three full-scale RBS sloped connections with the slope angle of 25° to study the effect of the sloping on the connection behavior. Hong [25] carried out a numerical study on RBS beam sloped connection to study the slope effect on the behavior of the building. Results showed that increasing slope angle cause stress concentration and should be less than 10° in order to be compatible with the prequalified connection details.

Literature review shows that characteristics of extended end-plate beam-to-column sloped connections need more investigations. So, in the present study, the performance of the four-bolted end-plate beam to column steel connection is investigated by considering various angles. Model assessment under four beam angles of 0, 10, 15, and 20 degrees relative to horizon is conducted. Finite element analyses have been done under cyclic loading in ABAQUS [26] software, and moment-rotation hysteresis, failure mechanisms, and bolts behavior are investigated.

2 Numerical study

The numerical model of extended end-plate connections is discussed in this section. The types and geometry of the specimens, software, modeling method, considered assumptions, and AISC limits are all explained. 3D finite element analysis of extended end-plate connections is conducted to evaluate the cyclic behavior of four specimens with various declinations.

2.1 Model characteristics

The details of the studied model taken from Shi et al. [27] are shown in Fig. 1 and Fig. 2 and Table 1. Eight bolts of the A572 type with the diameter of 20 mm are used in this investigation. Material properties of the bolt and steel including Young modulus, yield stress, and ultimate stress are provided in Table 2. Declination values of the beam are considered to be 0, 10, 15, and 20 to evaluate the behavior of extended end-plate connections. According to Fig. 1, column and beam lengths are 2300 and 1200 mm, respectively. Continuity plates, and stiffeners are used due to the force transferring process between beam and column, and tension concentration at the end of the beam (Fig. 3).

2.2 Analysis method

The behavior of the model is investigated in Abaqus [26] as a finite element analysis software. Model assessment is conducted by considering nonlinearity effects of materials.

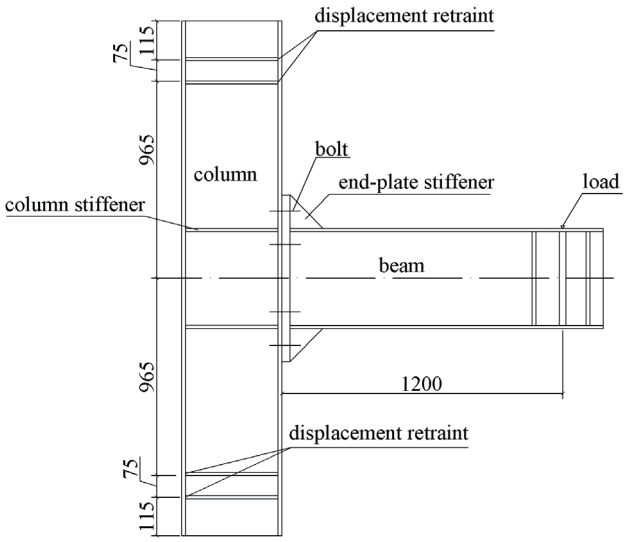

Fig. 1 The details of the perpendicular beam-to-column connection [27]

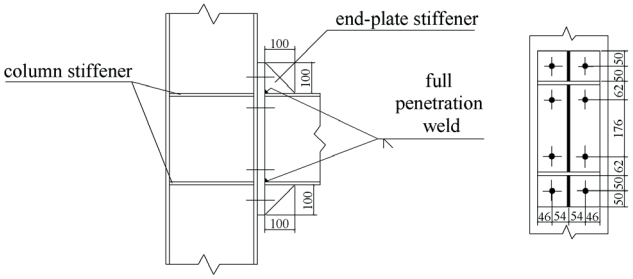

Fig. 2 The details of the connection parts [27]

Bolts were pre-tensioned and the time step of the analysis was assumed to be 0.01. Elements are connected by a complete penetration weld which is elastic and it is assumed that no failure will occur in the weld until ultimate state. It is necessary to define the interaction between the parts which are in contact with each other. For example, sections are directly connected to each other by the tie method.

Table 1 Details of the model

Element	Length (mm)	Width-flange (mm)	Height-web (mm)	Thickness (mm)	
				Flange	Web
Beam	1200	200	300	12	8
Column	2300	250	300	12	8
End-plate	500	200	-	10	-
Stiffener*	100	100	-	10	-

* The details of the stiffener plates are just for C1, and they will be changed by the changing of the connection angle

Table 2 Bolts and steel sections characteristics

Details	ST37 Sections	A572 Bolts
Young modulus (GPa)	210	210
Yield Stress (MPa)	240	350
Ultimate Stress (MPa)	360	450

But, for some surfaces, surface-to-surface contact was utilized with related contact property. The friction coefficient for tangential contact was considered to be 0.44, and hard contact was considered for normal contact. Boundary conditions were applied to pretend penetration effect between connection parts. This mechanism is considered for all adjacent sliding surfaces whereas other surfaces are tied.

Elements are meshed in the connection zone according to the structure volume and required accuracy. Due to the flat parts of the connection, hexagonal elements with eight nodes were used to model parts of the beam, column, stiffener plates, and bolts. The average dimensions of meshes in large parts such as a beam and column, and small parts such as bolts were 20 and 10 mm, respectively. Therefore, it is possible to assign nonlinearity of materials and large stresses and strains. It is worth mentioning that meshes at connection zone are compacted.

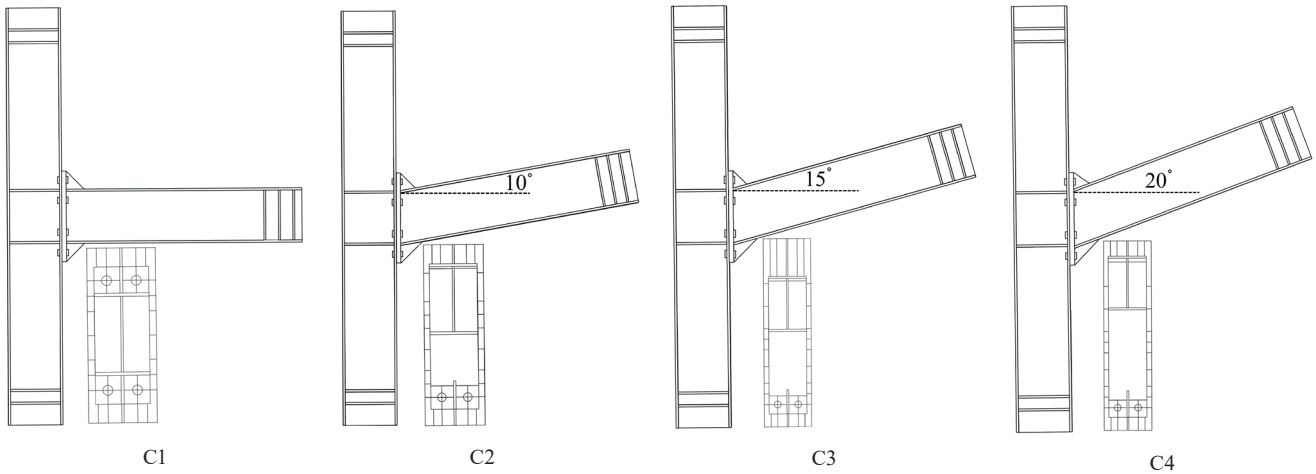

Fig. 3 Four connection types with various angles

Fig. 4 and Table 3 show details of the load pattern used in this study which is cyclic by considering benchmark load pattern of the codes. The load pattern contains the step including from 0.0375 radian peak deformation to 0.06 radian with various number of cycles. Rotation of the beam in beam-to-column connection zone ($\theta = \Delta/L$) was calculated based on the displacement of the end of the beam corresponding (Δ) to the length of the beam (L). Applied load and boundary conditions are shown in Fig. 1. As shown in Fig. 1, supports are restrained as fixed and beam rotation is considered to be up to 0.06. In order to make the boundary condition clear, Fig. 5 seems to be useful. According to AISC, extended end-plate beam-to-column connections in SMFs and IMFs should bear at least 0.04 and 0.02 radian rotation, respectively, under cyclic loading before reaching to their failure points.

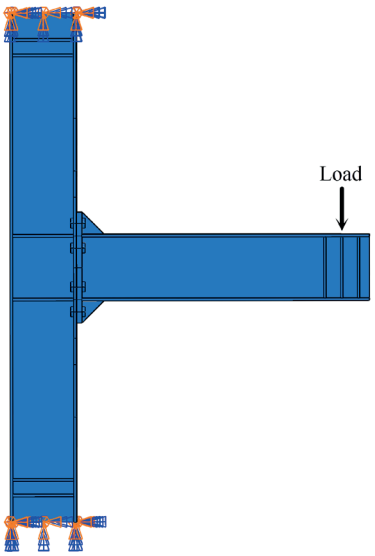

Fig. 5 Applied boundary condition in numerical study

2.3 Verification

In order to verify the finite element model in Abaqus [26], after modeling, the results were compared with the experimental model mentioned by Shi et al. [28]. Among the sections used by Shi et al. [28], SC5 is used for verifying the model. By applying a determined displacement which equals to 55 mm at the end of the beam, moment-rotation curve was obtained. In order to find appropriate mesh by considering not only accuracy but also efficient time, mesh sensitivity analysis was conducted on the model with the element size of 15, 20, 25, and 30 mm incorporated in Fig. 6. Based on the results, mesh with the size of 20 mm was utilized for the rest of the study to consider both accuracy and running time. By comparing the result of the FEA and experiment, almost 5% error can be seen in elastic part of moment rotation curve. It should be noted that this negligible error can be due to the experimental errors at the beginning of the loading, modeling errors in the FE software, or the value of Young modulus. Fig. 7 and Fig. 8 show the failure mode of the specimen in experimental and FE analysis seeming to be similar.

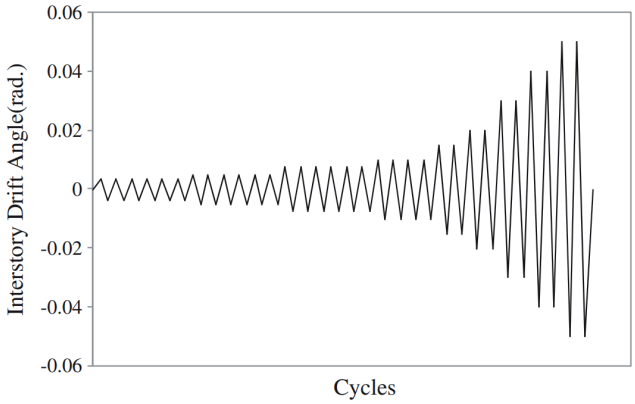

Fig. 4 FEMA loading time history

Table 3 FEMA cyclic loading characteristics

Load step	Peak deformation (rad)	Number of cycles
1	0.00375	6
2	0.0050	6
3	0.0075	6
4	0.010	4
5	0.015	2
6	0.020	2
7	0.030	2
8	0.040	2
9	0.05	2
10	0.06	2

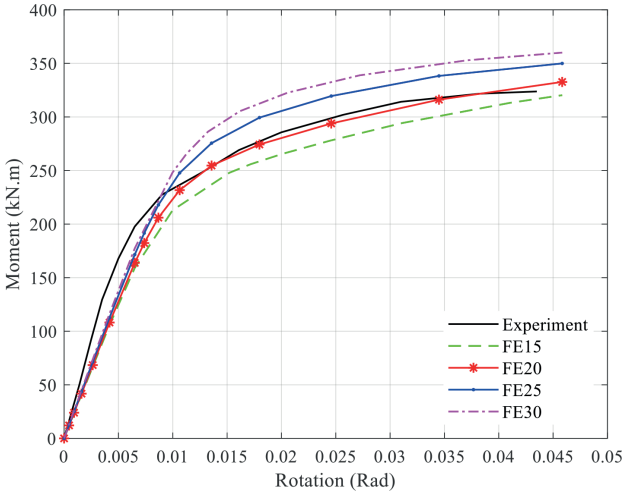

Fig. 6 Experimental and numerical moment-rotation comparison

(a) (b)

Fig. 7 a) Experimental specimen [28], b) Numerical specimen

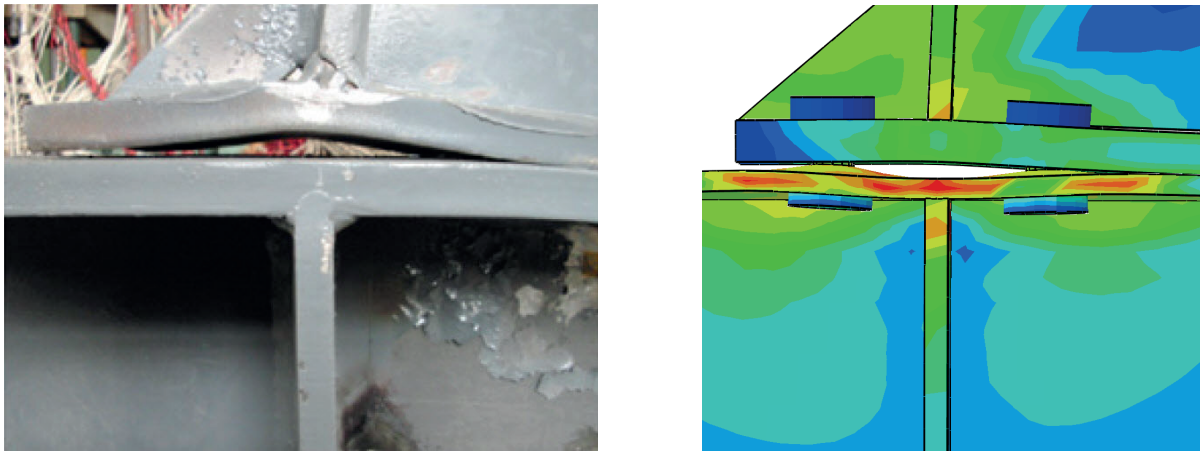

Fig. 8 Experimental [28] and numerical comparison of end-plate interaction with the column

3 Results

The behavior of the four specimens of the extended end-plate beam-to-column connections under cyclic loading is expressed in this section. Due to the AISC seismic limits in special moment frames with high ductility, beams moment value under the 0.04 rad rotation in the connection should be higher than 80% of plastic moment capacity of the beam. Moreover, the connection should not yield before reaching to 0.04 rad. Also, mentioned limitations are applicable to connections in intermediate moment frames with a beam rotation limit of 0.02 rad. Moment-rotation hysteresis curve, failure mechanism, and bolts behavior as the important components indicating the behavior of the structure will be represented as follows:

3.1 Moment-rotation hysteresis

Before studying the hysteresis behavior, the effect of the slope under monotonic loading on the connection behavior was studied. As it is clear in Fig. 9, by increasing the slope, the plastic and ultimate moment and rotation decreases. Moreover, the area under the curve indicating absorbed energy declines by increasing the slope. Therefore, increase in the slope results in decrease in the ductility.

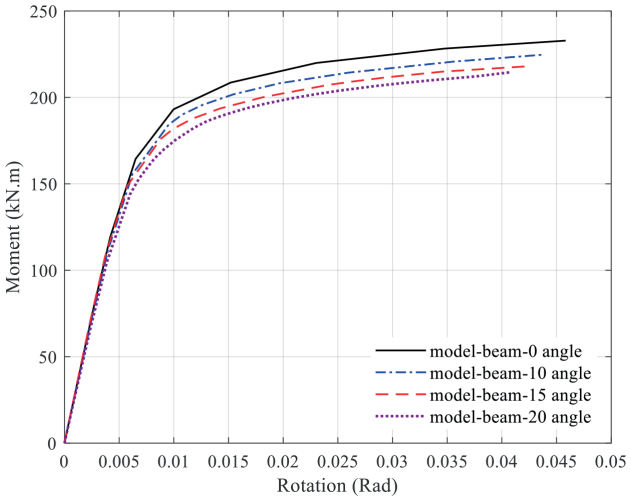

Fig. 9 Moment-rotation curve under monotonic load for various slopes

Moment rotation hysteresis loops corresponding to story drift for investigated specimens are depicted in Fig. 10. According to Fig. 10, values of the maximum moment occurred in the connections are 282.6, 272.7, 265, and 263 kN.m for specimen C1, C2, C3, and C4, respectively. The corresponding rotation which are 0.0423, 0.04, 0.04, and 0.045 rad with respect to the moments are provided in Fig. 10. Therefore, it can be concluded that connections satisfy the 0.04 rad rotation limitation, and results indicated that moment bearing capacity decreases when the beam angle increases as it is shown in Table 4. According to Table 4, although the beam angle in the specimen C4 is twice the C2, moment capacity is just reduced by 3.5% with respect to C2. As shown in Fig. 11, all the specimens can bear 0.04 drift before failure.

It can be observed that by increasing the beam angle, the slope of the curve decrease, and the area below the diagram decreases. Decrease in the area under the curve claims that the ductility of the structure decreases by angle increasing. Energy dissipation capacity has a direct relation with the area under moment-rotation hysteresis.

Table 4 Maximum moment comparison of numerical specimens

	C1	C2	C3	C4
Beam angle	0	10°	15°	20°
Moment bearing capacity (kN.m)	282.6	272.7	265	263
Moment bearing capacity reduction with respect to C1 (%)	-	3.5	6.2	6.7

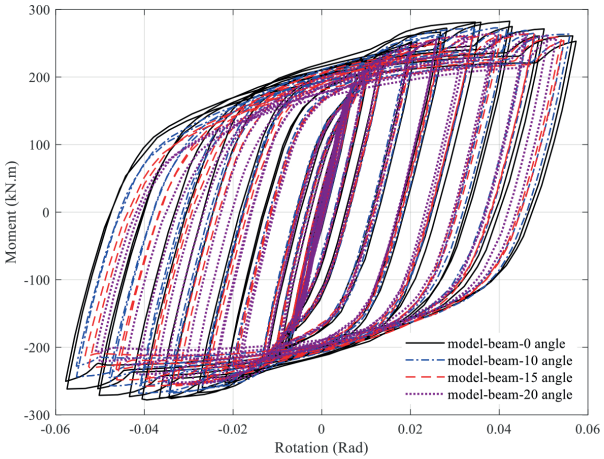

Fig. 11 Cyclic moment-rotation comparison of four sloped beam-to-column connection

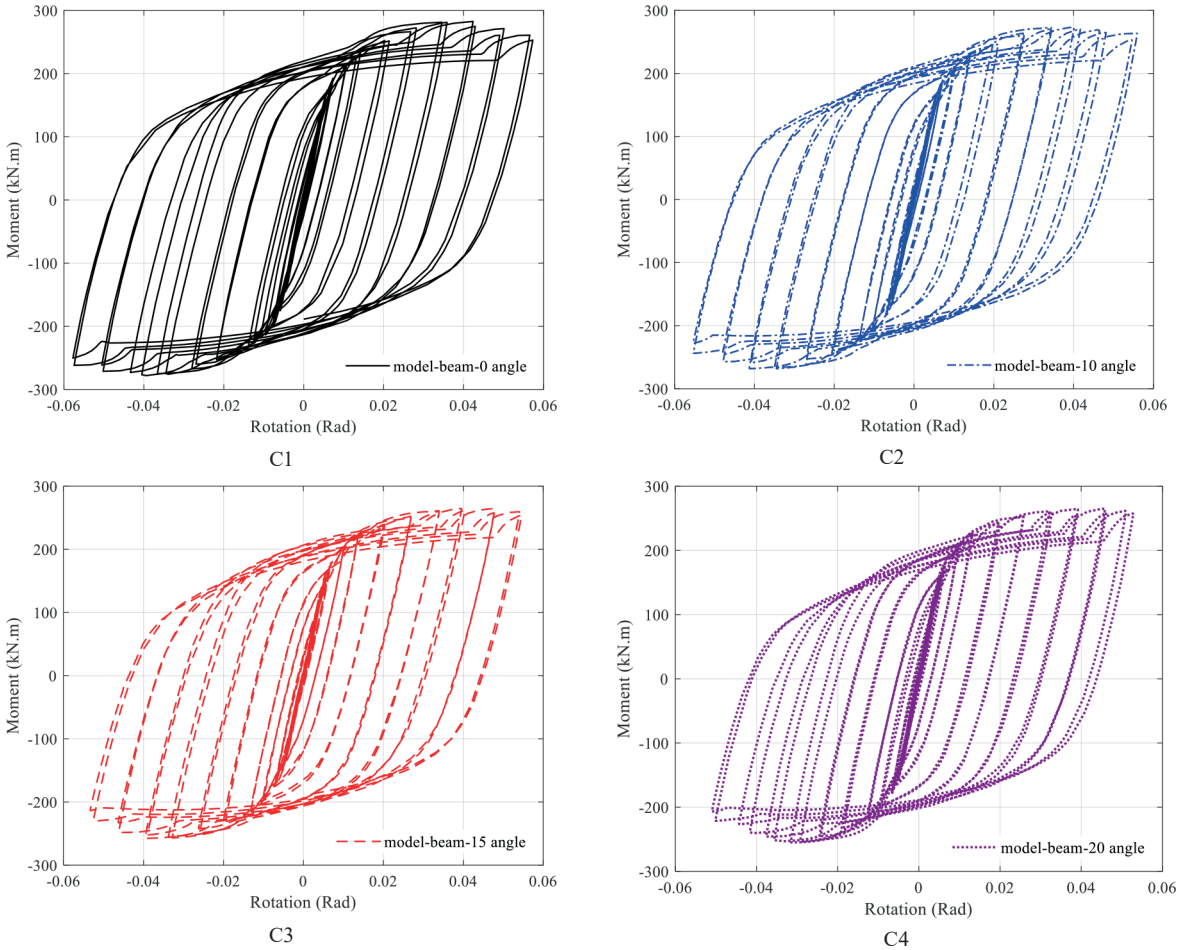

Fig. 10 Moment-rotation hysteresis of column surface for the specimens

The area under the moment-rotation hysteresis curve of the specimens C2, C3, and C4 are 8, 17, and 22 percent lower than C1, respectively. Generally, the reduction in the energy dissipation capacity is because of the stress concentration in sloped connections.

3.2 Failure mechanism

Failure mechanisms of the modeled beam-to-column connections are shown in Fig. 12. According to Fig. 12, by increasing the slope, the possibility of the failure in the stiffness decreases and the end part of the beam bears much stress. It is also observed that in failure regions, the yielding stress of the steel exceeds 24 MPa at the end of loading for all the specimens. In specimen C1 based on Fig. 12, connection failure started from stiffeners and continued to end-plates and column flange. The failure mechanism in specimen C2 is similar to C1 but the internal force of stiffeners is 3% lower than C1. Internal force of the stiffener and column flange in specimen C3 is decreased by 6.5% with respect to C1 because of the decrease in moment as shown in Fig. 12. In specimen C4 the internal force of the stiffener is 2% lower than C1 but the upper part of the beam experiences a stress concentration increase which is similar to C3 as indicated in Fig. 12.

As depicted in Fig. 13, the stress of stiffeners is 360 Mpa. It should be noted that by increasing the slope, stiffener location experiences maximum stress changing from bottom stiffener to the upper one. Moreover, by increasing the slope, the stiffener changes from right-angled condition to oblique angles resulting in non-uniform stress distribution

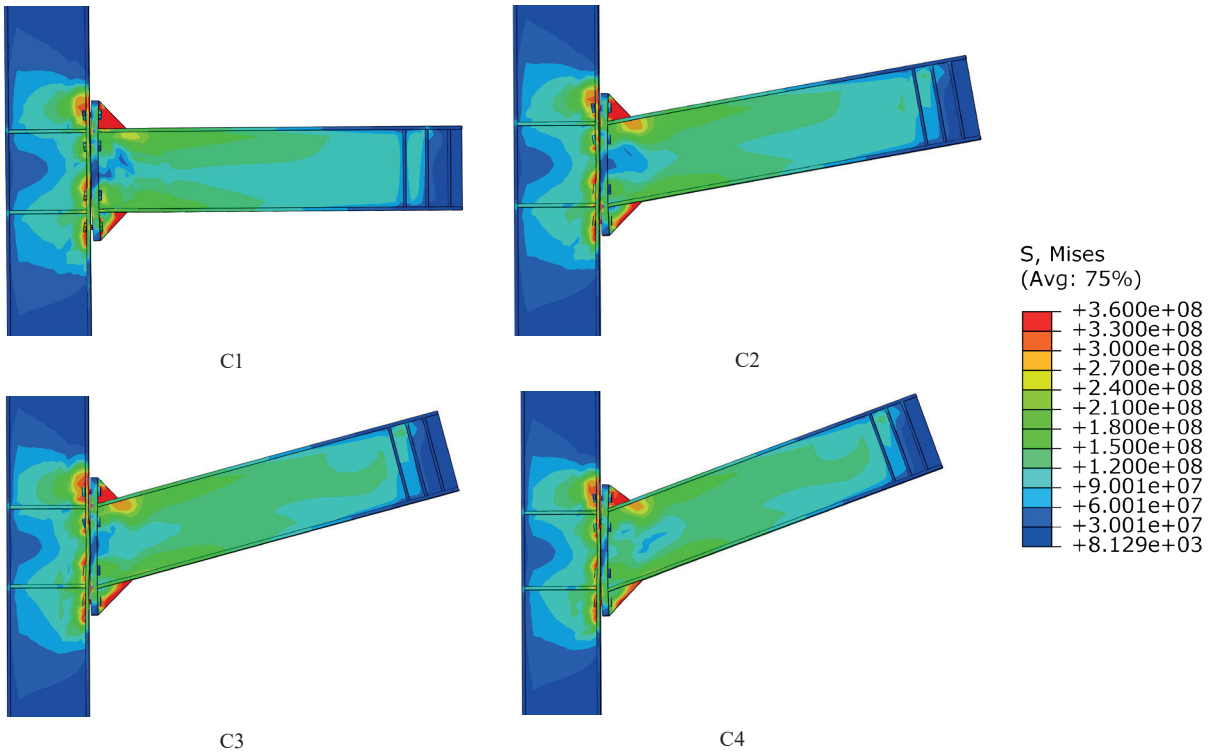

Fig. 12 Failure mechanisms of the specimens

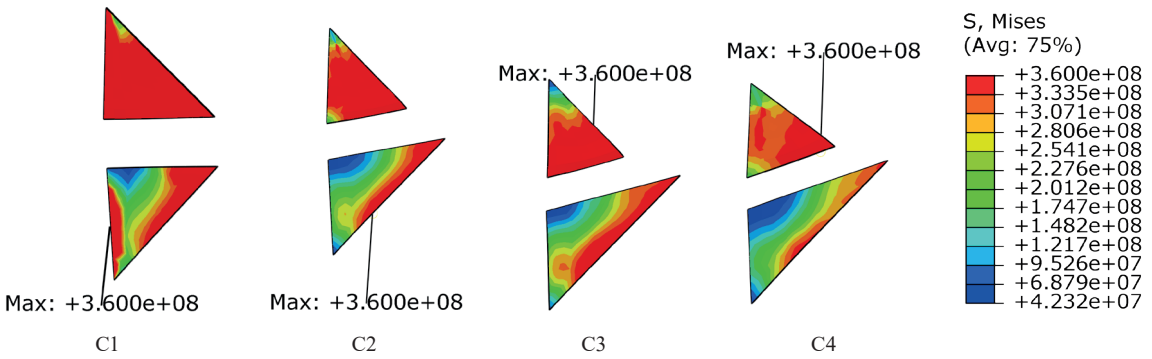

Fig. 13 Failure mechanisms of the stiffeners

in the stiffener causing extra stress concentration in the beam flange. Also, due to increasing stress distribution in the upper stiffener and decreasing in the lower one, the amount of stress concentration increases and decreases in the upper and lower beam flange, respectively.

3.3 Behavior of the bolts

In this part, the behavior of the bolts in specimens is illustrated. Fig. 14 shows that the bolts' stress remains constant by increasing the slope, but in specimen C1 and C2, one of the bolts of the upper row is critical while critical bolts of specimen C3 and C4 are in bottom row exactly opposite of the stiffener plates. Bolts' type is A572 with yield and ultimate stresses of 350 and 450 MPa, respectively. Critical states of the bolts considering maximum stress are depicted in Fig. 14. Bolts' results provided in Fig. 14 shows that despite constant value of the maximum stress, stress distribution is different for all the test states. Also, none of the bolts reached to their ultimate state.

4 Conclusions

In this article, the effect of the connection angle in the extended end-plate beam-to-column connections was investigated under cyclic loadings. The evaluation contains four beam-to-column connection specimens which were investigated under various slope angles. Moment-rotation hysteresis, failure mechanism, and behavior of the bolts were the main focus of the present study to investigate the behavior of the sloped extended end-plate beam-to-column connections.

Sloped connections were able to bear 0.04 rad rotation before failure as mentioned in the design guides. The rotation value for the sloped connections were 0.0423, 0.04, 0.04, and 0.045 rad, respectively. Increasing the value of the slope caused the maximum moment bearing capacity to decrease to the value of 19.6 kN.m. Therefore, the maximum moment bearing capacity decreased about 0.98 kN.m for each increment in the degree. Due to slope increasing, the ductility of the structure decreased 8%, 17%, and 22% for the specimens C2, C3, and C4 in comparison with specimen C1, respectively, because of the area reduction under the moment-rotation curve. Due to the increase of the value of the connection slope, the moment-rotation diagram slope was decreased showing bearing capacity degradation of the connection. Any variation in extended end-plate beam-to-column connection angle under cyclic loading did not lead to a considerable increase of the stress of the bolt, but the maximum stress position of the bolt changed from the upper row to the lower one by increasing the slope. Failure process of the connection in specimens with low slope started in stiffeners and stresses decreased by increasing the slope.

In general, based on the results, sloped extended end-plate connections are able to be used in steel structures, but due to the stress concentration, slopes more than 10° are note suggested to be used. Also, slopes do not have an effect on the bolt behavior. Moreover, it can be suggested that by increasing the slope, the thickness of the stiffeners needs to be increased to behave well.

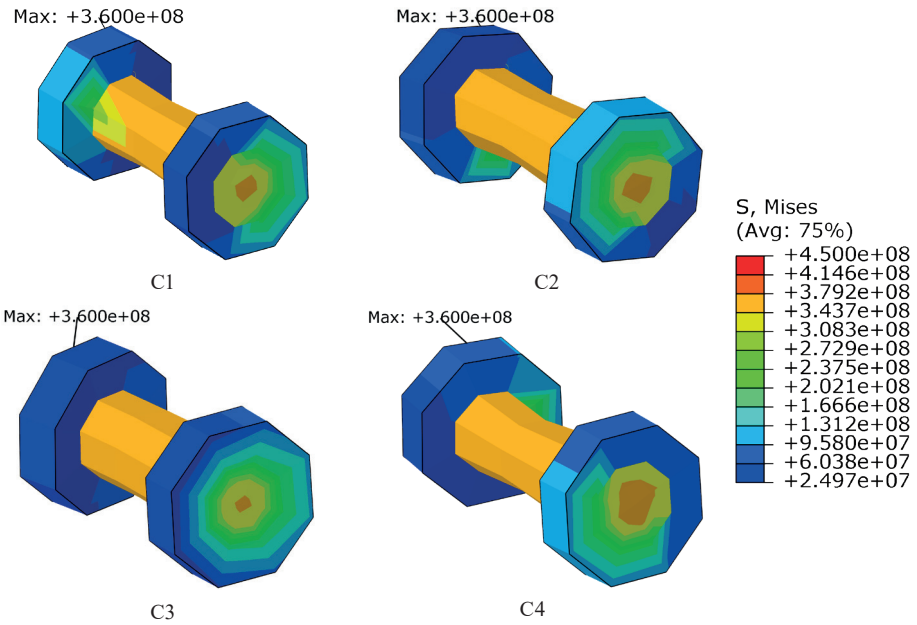

Fig. 14 Maximum stress of bolts

References

[1] Engelhardt, M. D., Husain, A. S. "Cyclic tests on large scale steel moment connections", In: Proceedings of the Tenth World Conference on Earthquake Engineering, Madrid, Spain, 1992, pp. 2285–2290. ISBN 90 5410 0605

[2] ElSabbagh, A., Sharaf, T., Nagy, S., ElGhandour, M. "Behavior of extended end-plate bolted connections subjected to monotonic and cyclic loads", Engineering Structures, 190, pp. 142–159, 2019. https://doi.org/10.1016/j.engstruct.2019.04.016

[3] Miller, D. K. "Lessons learned from the Northridge earthquake", Engineering Structures, 20(4), pp. 249–260, 1998. https://doi.org/10.1016/S0141-0296(97)00031-X

[4] Chen, C.-C., Chen, S.-W., Chung, M.-D., Lin, M.-C. "Cyclic behaviour of unreinforced and rib-reinforced moment connections", Journal of Constructional Steel Research, 61(1), pp. 1–21, 2005. https://doi.org/10.1016/j.jcsr.2004.06.005

[5] Ghindea, M., Ballok, R. "State-of-the-art review on bolted steel beam-to-column connections", Bulletin of the Transilvania University of Braşov, 8(57), pp. 91–98, 2015.

[6] ANSI/AISC "Prequalified Connections for Special and Intermediate Steel Moment Frames for Seismic Applications (ANSI/AISC 358-16)", American Institute of Steel Construction, Chicago, IL, USA, 2016.

[7] Lee, Y. H., Tan, C. S., Mohammad, S., Md Tahir, M., Shek, P. N. "Review on cold-formed steel connections", The Scientific World Journal, 2014, 951216, 2014. https://doi.org/10.1155/2014/951216

[8] Aksoylar, N. D., Elnashai, A. S., Mahmoud, H. "The design and seismic performance of low-rise long-span frames with semi-rigid connections", Journal of Constructional Steel Research, 67(1), pp. 114–126, 2011. https://doi.org/10.1016/j.jcsr.2010.07.001

[9] Feizi, M. G., Mojtahedi, A., Nourani, V. "Effect of semi-rigid connections in improvement of seismic performance of steel moment-resisting frames", Steel and Composite Structures, 19(2), pp. 467–484, 2015. https://doi.org/10.12989/scs.2015.19.2.467

[10] Meng, B., Zhong, W., Hao, J., Song, X. "Improving anti-collapse performance of steel frame with RBS connection", Journal of Constructional Steel Research, 170, 106119, 2020. https://doi.org/10.1016/j.jcsr.2020.106119

[11] Ghaderi, M., Gerami, M., Vahdani, R. "Performance assessment of bolted extended end-plate moment connections constructed from grade St-37 steel subjected to fatigue", Journal of Materials in Civil Engineering, 32(5), 04020092, 2020. https://doi.org/10.1061/(asce)mt.1943-5533.0003066

[12] Solhmirzaei, A., Tahamouli Roudsari, M., Hosseini Hashemi, B. "A new detail for the panel zone of beam-to-wide flange column connections with endplate", Structures, 34, pp. 1108–1123, 2021. https://doi.org/10.1016/j.istruc.2021.08.061

[13] Masoudi, M. J., Broumand, P. "Seismic performance of welded flange plate (WFP) connections in composite steel structures", Journal of Constructional Steel Research, 189, 107103, 2022. https://doi.org/10.1016/j.jcsr.2021.107103

[14] Krishnamurthy, N. "A fresh look at bolted end-plate behavior and design", Engineering Journal, 15(2), pp. 39–49, 1978.

[15] Ghassemieh, M., Kukreti, A. R., Murray, T. M. "Inelastic finite element analysis of stiffened end-plate moment connections", University of Oklahoma, Norman, OK, USA, Rep. FSEL/AISC 83–02, 1983.

[16] Adey, B. T., Grondin, G. Y., Cheng, J. "Extended end plate moment connections under cyclic loading", Journal of Constructional Steel Research, 46(1–3), pp. 435–436, 1998.

[17] Sumner, E. A., Murray, T. M. "Behavior of Extended End-Plate Moment Connections Subject to Cyclic Loading", Journal of Structural Engineering, 128(4), pp. 501–508, 2002. https://doi.org/10.1061/(asce)0733-9445(2002)128:4(501)

[18] Díaz, C., Victoria, M., Martí, P., Querin, O. M. "FE model of beam-to-column extended end-plate joints", Journal of Constructional Steel Research, 67(10), pp. 1578–1590, 2011. https://doi.org/10.1016/j.jcsr.2011.04.002

[19] Dessouki, A. K., Youssef, A. H., Ibrahim, M. M. "Behavior of I-beam bolted extended end-plate moment connections", Ain Shams Engineering Journal, 4(4), pp. 685–699, 2013. https://doi.org/10.1016/j.asej.2013.03.004

[20] Yang, J.-G., Kim, Y.-B., Kwak, M. "Evaluation of the Energy Dissipation Capacities of Beam-to-Column Moment Connections for Steel Frames", Journal of Asian Architecture and Building Engineering, 15(3), pp. 573–579, 2016. https://doi.org/10.3130/jaabe.15.573

[21] di Sarno, L., Paolacci, F., Sextos, A. G. "Seismic performance assessment of existing steel buildings: a case study", Key Engineering Materials, 763, pp. 1067–1076, 2018. https://doi.org/10.4028/www.scientific.net/kem.763.1067

[22] Yilmaz, O., Bekiroğlu, S. "Seismic performance of post-northridge welded connections", Latin American Journal of Solids and Structures, 15(2), e18, 2018. https://doi.org/10.1590/1679-78254574

[23] Llanes-Tizoc, M. D., Reyes-Salazar, A., Ruiz, S. E., Valenzuela-Beltrán, F., Bojorquez, E., Chávez, R. "Reliability analysis of steel buildings considering the flexibility of the connections of the GFs", Structures, 27, pp. 2170–2181, 2020. https://doi.org/10.1016/j.istruc.2020.08.014

[24] Mashayekh, A., Uang, C.-M. "Cyclic Response of Sloped Steel Moment Connections", Journal of Structural Engineering, 145(7), 04019058, 2019. https://doi.org/10.1061/(asce)st.1943-541x.0002339

[25] Hong, J.-K. "Sloped RBS Moment Connections at Roof Floor Subjected to Cyclic Loading: Analytical Investigation", International Journal of Steel Structures, 19(1), pp. 329–339, 2019. https://doi.org/10.1007/s13296-018-0198-4

[26] Dassault Systemes Simulia Corp "Abaqus 2018", [online] Available at: https://www.3ds.com/

[27] Shi, G., Shi, Y., Wang, Y., Bradford, M. A. "Numerical simulation of steel pretensioned bolted end-plate connections of different types and details", Engineering Structures, 30, pp. 2677–2686, 2008. https://doi.org/10.1016/j.engstruct.2008.02.013

[28] Shi, Y., Shi, G., Wang, Y. "Experimental and theoretical analysis of the moment–rotation behaviour of stiffened extended end-plate connections", Journal of Constructional Steel Research, 63(9), pp. 1279–1293, 2007. https://doi.org/10.1016/j.jcsr.2006.11.008